Immunology
The Journal of cells, molecules, systems and technologies

British Society for immunology

IMMUNOLOGY ORIGINAL ARTICLE

A novel pathogenic RBP-3 peptide reveals epitope spreading in persistent experimental autoimmune uveoretinitis

Joanne Boldison,[1] Tarnjit K. Khera,[2] David A. Copland,[2] Madeleine L. Stimpson,[2] Gemma L. Crawford,[2] Andrew D. Dick[1,2] and Lindsay B. Nicholson[1,2]

[1]*School of Cellular and Molecular Medicine, University of Bristol, Bristol, and* [2]*Academic Unit of Ophthalmology, School of Clinical Sciences, University of Bristol, Bristol, UK*

doi:10.1111/imm.12503
Received 12 April 2015; accepted 29 June 2015.
Correspondence: Dr Lindsay Nicholson, School of Cellular and Molecular Medicine, University of Bristol, University Walk, Bristol BS8 1TD, UK.
Email: l.nicholson@bristol.ac.uk
Senior author: Lindsay B. Nicholson

Summary

Experimental autoimmune uveoretinitis (EAU) in the C57BL/6J mouse is a model of non-infectious posterior segment intraocular inflammation that parallels clinical features of the human disease. The purpose of this study was to analyse the immune response to the four murine subunits of retinol binding protein-3 (RBP-3) to identify pathogenic epitopes to investigate the presence of intramolecular epitope spreading during the persistent inflammation phase observed in this model of EAU. Recombinant murine subunits of the RBP-3 protein were purified and used to immunize C57BL/6J mice to induce EAU. An overlapping peptide library was used to screen RBP-3 subunit 3 for immunogenicity and pathogenicity. Disease phenotype and characterization of pathogenic subunits and peptides was undertaken by topical endoscopic fundal imaging, immunohistochemistry, proliferation assays and flow cytometry. RBP-3 subunits 1, 2 and 3 induced EAU in the C57BL/6J mice, with subunit 3 eliciting the most destructive clinical disease. Within subunit 3 we identified a novel uveitogenic epitope, 629–643. The disease induced by this peptide was comparable to that produced by the uveitogenic 1–20 peptide. Following immunization, peptide-specific responses by $CD4^+$ and $CD8^+$ T-cell subsets were detected, and cells from both populations were present in the retinal inflammatory infiltrate. Intramolecular epitope spreading between 629–643 and 1–20 was detected in mice with clinical signs of disease. The 629–643 RBP-3 peptide is a major uveitogenic peptide for the induction of EAU in C57BL/6J mice and the persistent clinical disease induced with one peptide leads to epitope spreading.

Keywords: autoimmunity; chronic inflammation; epitope spreading; retina; uveitis.

Introduction

Experimental autoimmune uveoretinitis (EAU) is an antigen-specific $CD4^+$ T-cell-dependent model of non-infectious intraocular inflammation. Animal models have proven useful in probing cellular mechanisms of disease and as a pre-clinical model to develop treatments for human uveitis.[1] More recently in parallel with features of human disease cell flux, persistence and chronic tissue changes such as angiogenesis have been reported in murine EAU.[2,3] In the C57BL/6 (H-2^b) mouse model of EAU, immunization with either the human sequence 1–20 or the murine sequence 1–16 of the retinol binding protein-3 (RBP-3; also known as interphotoreceptor retinoid-binding protein) peptide and adjuvants induces EAU, predominantly focused within the posterior segment of the eye.[4–6] Chronic changes in the tissue have important implications for human disease[7] but the mechanisms regulating persistence and evidence for epitope spreading in this model remain elusive.

Retinol binding protein-3 is a key protein in establishing ocular immune tolerance and plays a functionally

Abbreviations: EAU, experimental autoimmune uveoretinitis; RBP-3, retinol binding protein-3; 7-AAD, 7-aminoactinomycin D; OVA, ovalbumin; TEFI, topical endoscopic fundal imaging

significant role in EAU as shown by early studies, which demonstrated that the expression level of retinal antigens in the thymus correlates with EAU susceptibility.[8] Later work found that RBP-3 expression in the thymus is modulated by AIRE (autoimmune regulator) and the loss of expression of RBP-3 alone is sufficient to confer susceptibility to spontaneous ocular autoimmunity.[9] Furthermore, the transfer of uveitogenic T cells from RBP-3 knockout animals reveals the importance of RBP-3 in shaping the T-cell repertoire.[10]

Strain-to-strain variability in mouse models of EAU has been reported extensively, and is partly dependent on MHC type.[11] In EAU in the C57BL/6J (H-2^b) strain, the human peptide RBP-3 1–20 is the most widely used uveitogenic epitope.[4] Other pathogenic epitopes, such as residues 461–480 (subunit 2) and 651–670 (subunit 3) of RBP-3, have also been reported[12] in studies that used bovine RBP-3 protein for immunization and a peptide library based on human RBP-3 for screening. Although there is an 80% homology between bovine and human RBP-3, amino acid differences may affect the identification of novel pathogenic epitopes and our ability to illuminate whether epitope spreading occurs.

The powerful effects of RBP-3 on shaping tolerance led us to study immune responses to immunization with recombinant murine proteins. We characterized responses to the four RBP-3 subunits and identified a novel murine epitope that induced disease. This pathogenic peptide 629–643 (of subunit 3) has similar disease-inducing potential and potency as 1–20 peptide, and immunization with either peptide leads to epitope spreading to the second.

Materials and methods

Mice

C57BL/6J mice were originally obtained from Harlan UK Limited (Oxford, UK) and breeding colonies were established within the Animal Services Unit at Bristol University, Bristol, UK. Mice were housed in specific pathogen-free conditions with continuously available water and food. Female mice immunized for disease induction were aged between 6 and 8 weeks. All mice were kept in the animal house facilities of the University of Bristol, according to Home Office Regulations. Treatment of animals conformed to UK legislation and to the ARVO statement for the Use of Animals in Ophthalmic and Vision research. All strains used were screened to confirm that they were negative for the rd8 mutation.[13]

Reagents

Human RBP-$3_{1–20}$ Peptide (GPTHLFQPSLVLDMAKV LLD) and chicken ovalbumin (OVA) (ISQAVHAAHAEIN EAGR) were synthesized by Sigma-Aldrich (Poole, UK). Murine RBP-$3_{629–643}$ (EAHYARPEIAQRARA) and the peptide library were synthesized by Severn Biotech (Worcestershire, UK). Peptide purity was > 95% as determined by HPLC. Complete medium consisted of RPMI-1640 media supplemented with 10% heat inactivated fetal calf serum, 100 U/ml penicillin-streptomycin, 2 mmol/l L-glutamine and 5×10^{-5} mol/l 2-mercaptoethanol (Life Technologies, Paisley, UK).

RBP-3 recombinant subunits

Recombinant histidine-tagged proteins were produced from *Escherichia coli* containing murine RBP-3 subunit 1, 2, 3 or 4 constructs. Briefly, total RNA was isolated from the eyes of C57BL/6J mice (H-2^b) by Trizol® (Invitrogen, Paisley, UK). RNA was converted to cDNA using the Reverse Transcriptase reaction from Invitrogen, then amplified using KOD DNA polymerase (Novagen, Nottingham, UK). PCR fragments were cloned into the Gateway entry vector pCR® 8/GW/TOPO using the pCR®/GW/TOPO TA Cloning kit (Invitrogen) according to the manufacturer's instructions. Entry clone plasmids with the correct insert were transformed into library efficient® DH5α cells (Invitrogen). Plasmid of the pDEST17 expression clone was transformed into the host expression system BL21-AI™ cells (Invitrogen). All inserts were sequenced to ensure the correct orientation (Eurofins MWG operons).

Protein purification

Escherichia coli containing recombinant expression plasmids were grown in Luria–Bertani growth media (Media Services, Bristol University) at 37° at 180 rpm to an optical density at 600 nm of 0·35 before the addition of isopropyl-β-D-thiogalactopyranoside (Life Technologies) to induce protein expression. Isopropyl-β-D-thiogalactopyranoside (1·5 mM) was added for 3 hr before centrifuging bacterial cultures at 800 g for 20 min at 4°. Cells were lysed by cell disruption (Constant Systems Ltd, Daventry, UK). The disrupted material was centrifuged at 800 g for 20 min at 4°. Subunits 1, 2 and 3 were expressed in inclusion bodies and solubilized in 6 M guanidine hydrochloride but as subunit 4 was soluble it was resuspended in native binding buffer (Invitrogen). Protein was loaded onto a Probond Nickel Chelating Column according to manufacturer's instructions (Invitrogen). The purified proteins were renatured by using a PD-10 desalting column (GE Healthcare, Buckinghamshire, UK). Each fraction was analysed by SDS–PAGE and concentration was determined by absorbance at 280 nm on a spectrophotometer or by bicinchoninic acid assay.

EAU induction

C57BL/6J mice were immunized subcutaneously in one flank with equimolar amounts (230 nmol) of either 1–20

(500 μg) or 629–643 (400 μg) RBP-3 peptide in water (2% DMSO), 50 μg of RBP-3 recombinant subunit proteins or 200 μg of peptide library proteins, emulsified in complete Freund's adjuvant (1 mg/ml; 1 : 1 volume/volume) supplemented with 1·5 mg/ml *Mycobacterium tuberculosis* complete H37 Ra (BD Biosciences, Oxford, UK), and 1·5 μg *Bordetella pertussis* toxin (Tocris, Bristol, UK) was given intraperitoneally.

Clinical assessment by topical endoscopic fundal imaging

Photographs were taken of the retina using a previously described method.[14] Fundal images were scored for inflammatory changes of the optic disc, retinal vessels, retinal lesions and structural damage; all scores were added together to make a final disease score. This clinical grading system was adapted from ref. 15 and has been previously published.[16] Scoring was carried out independently by trained assessors for whom the origin of the data was masked.

Immunohistochemistry

Immunohistochemistry was performed as previously described.[14] Briefly, eyes were removed from animals and embedded in optimal cutting temperature (RA Lamb) compound and snap frozen. Serial 12-μm cryostat sections were cut before staining with rat anti-mouse CD45 monoclonal antibody (Serotec, Oxford, UK), counterstained with haematoxylin (ThermoShandon, Pittsburgh, PA) and scored for inflammatory infiltrate.[14]

Cell preparations

Spleens were disrupted mechanically through a 40-μm cell strainer and red blood cells were lysed. Eyes were enucleated and carefully cleaned to remove all extraneous connective and vascular tissue. The retinas (including the ciliary body) were microscopically dissected in Hanks' balanced salt solution medium supplemented with 5% fetal calf serum. Retinal tissue was homogenized and mashed through a 40-μm cell strainer with a syringe plunger, to obtain a single cell suspension and stained for flow cytometry analysis. Quantification of the number of cells per eye has been described previously.[2]

Flow cytometry

Cell suspensions were incubated with 24G2 cell supernatant (Fc block) for 10 min at 4°. Cells were then stained with fluorochrome-conjugated monoclonal antibody against cell surface markers for 20 min at 4°. Multiparameter flow cytometry was carried out using different fluorochromes all purchased from BD Biosciences. Cells were resuspended in 7-aminoactinomycin D (7AAD), and dead cells excluded from analysis by gating on 7AAD-negative cells. Individual events were then acquired on a flow cytometer (LSR II, FACSDiva software; BD cytometry systems Oxford, UK). All analyses were performed using FlowJo software (Tree Star, Ashland, OR). The numbers of cells were calculated by reference to a known standard curve.[2]

Proliferation assays

Cells were seeded in triplicate at 1×10^5 per well in a 96-well round-bottom plate and cultured in complete medium containing 10 μg/ml of relevant peptide. Cells were cultured in a humidified environment at 37°C and 5% CO_2. Proliferation was measured by pulsing with 18·5 kBq [^{3}H]thymidine (Perkin Elmer, Waltham, MA) per well for 16 hr before being harvested onto 96-well filter mats with a 96-well harvester (Tomtec, Hamden, CT) and thymidine uptake (counts/min) was determined. Proliferation was also measured by CFSE (Carboxyfluorescein succinimidyl ester) staining; cells were stained with 0·5 μM CFSE and cultured for 96 hr before flow cytometry analysis. Proliferation was expressed as the fraction of divided cells as a percentage of the total.

ELISA

Murine interferon-γ (IFN-γ) and interleukin-17 (IL-17) production in culture supernatants was determined by sandwich ELISA. Briefly, capture antibodies (IFN-γ; IL-17) were applied in carbonate buffer (pH 9·6) to NUNC-Immuno plates (VWR, Lutterworth, UK) and incubated overnight at 4°C. Non-specific binding was blocked with 1% BSA in PBS for 1 hr at room temperature, and plates were then incubated with culture supernatants and recombinant protein standards for 2 hr. Detection antibody (IFN-γ; IL-17) was added for 1 hr at room temperature, followed by ExtrAvidin-Peroxidase (Sigma-Aldrich, Dorset, UK) for 30 min. TMB (Tetramethylbenzidine) substrate solution (BD Biosciences) was used for chromogen development, and the reaction was stopped using 2N H_2SO_4. The optical densities were read at 4.5×10^{-7} m with a reference filter of 5.95×10^{-7} mm and IFN-γ and IL-17 concentrations were determined from standard curves.

Statistical analyses

Data when paired were analysed by Wilcoxon matched pairs signed rank test and considered significant when results had a P-value of $\leq 0{\cdot}05$. When more than one variable was analysed, comparisons were made using analyses of variance (Kruskal–Wallis) and considered significant when results had a P-value of $\leq 0{\cdot}05$. To assess correlation a non-parametric Spearman's correlation test was used and considered significant when results had a

P-value of $\leq 0{\cdot}05$. All graphs and statistical tests were performed using GraphPad prism (GraphPad Software Inc., San Diego, CA).

Results

Recombinant RBP-3 subunits 1, 2 and 3 induce EAU

Groups of C57BL/6J mice were immunized with either 50 μg recombinant RBP-3 subunits 1, 2, 3 or 4, or 500 μg of RBP-3 1–20. The clinical disease course was monitored by topical endoscopic fundal imaging. Groups of mice immunized with RBP-3 subunit 1, 2 or 3 developed clinical EAU; however, no clinical disease was observed following immunization with RBP-3 subunit 4. Figure 1 shows representative fundal images and immunohistochemical staining with anti-CD45 antibody for each disease group. Clinical disease in the RBP-3 peptide 1–20 group was as previously described[3,4] and was confirmed by histology showing a disrupted retinal morphology and inflammatory infiltrate (white arrows). RBP-3 subunits 1 and 2 induced similar inflammation localizing to the optic disc and retinal vessels (vasculitis), corroborated by histology, which demonstrated retinal folds and $CD45^+$ cells (white arrows). In the group immunized with RBP-3 subunit 3 fundal photography showed a pronounced destructive pan-retinal inflammation with confluent lesions (Fig. 1, subunit 3). Furthermore, histological staining revealed extensive disruption of the photoreceptor layer characterized by large areas of $CD45^+$ infiltrate (subunit 3).

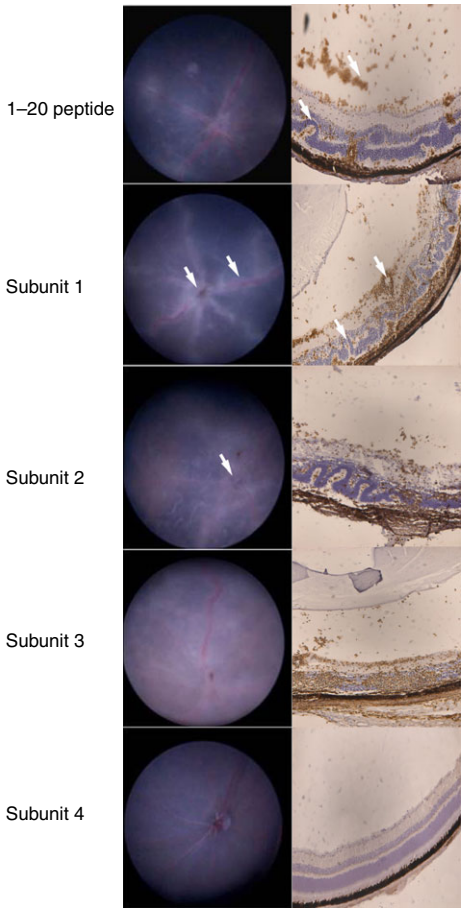

Figure 1. Retinol binding protein-3 (RBP-3) recombinant subunits induce experimental autoimmune uveoretinitis (EAU). C57BL/6J mice were immunized with either 50 μg/ml RBP-3 recombinant subunits 1, 2, 3, 4 or 500 μg/ml 1–20 RBP-3 peptide to induce EAU. Representative topical endoscopic fundal imaging (TEFI) and histology images are shown demonstrating clinical appearance, cellular infiltrate and structural morphology of the retina (vasculitis in the clinical pictures and $CD45^+$ cell infiltrate in the tissue sections are indicated by white arrows). TEFI images taken between days 23 and 25, mice were then killed before the eyes were enucleated, sectioned and stained for $CD45^+$ infiltrate.

Recombinant RBP-3 subunit 3 induces a severe form of EAU

In light of the extensive destruction that immunization with RBP-3 recombinant subunit 3 induced, we characterized this in more detail, by clinical and histological grading and quantification of cellular infiltrate, as previously reported.[14] Subunit 3 induced clinical disease of significantly greater severity ($P < 0{\cdot}01$) compared with disease induced by RBP-3 1–20, with RBP-3 subunit 1 inducing intermediate disease. This finding was corroborated by immunohistochemical assessment (Fig. 2b), which demonstrated more severe disease in the retinas of animals immunized with recombinant subunits compared with peptide 1–20. Quantification of $CD45^+$ leucocytes in the retina by flow cytometry showed comparable total cell infiltrate in all groups (Fig. 2c,d), greatest in animals immunized with subunit 3. Together these data pointed to the presence of a pathogenic epitope or epitopes within subunit 3. As the severity of disease induced by this subunit was greater than that previously reported for the non-immunodominant peptide 651–670,[12] this raised the possibility that additional epitopes might be present.

RBP-3 peptide library reveals new pathogenic epitopes

To complete an unbiased analysis of peptide responses within subunit 3, a peptide library based on the murine sequence[17,18] comprising a panel of 48 peptides spanning the subunit, 13 amino acids in length and with a five-amino-acid overlap, was constructed. Immunodominant epitopes were revealed by recall assays on splenocytes from RBP-3 subunit 3 immunized mice (data not shown). Responses higher than twice the background counts/min were considered meaningful (10 570 counts/min). Peptides were also analysed to identify those that contained $H\text{-}2^b$ binding motifs.[6] Peptides with binding

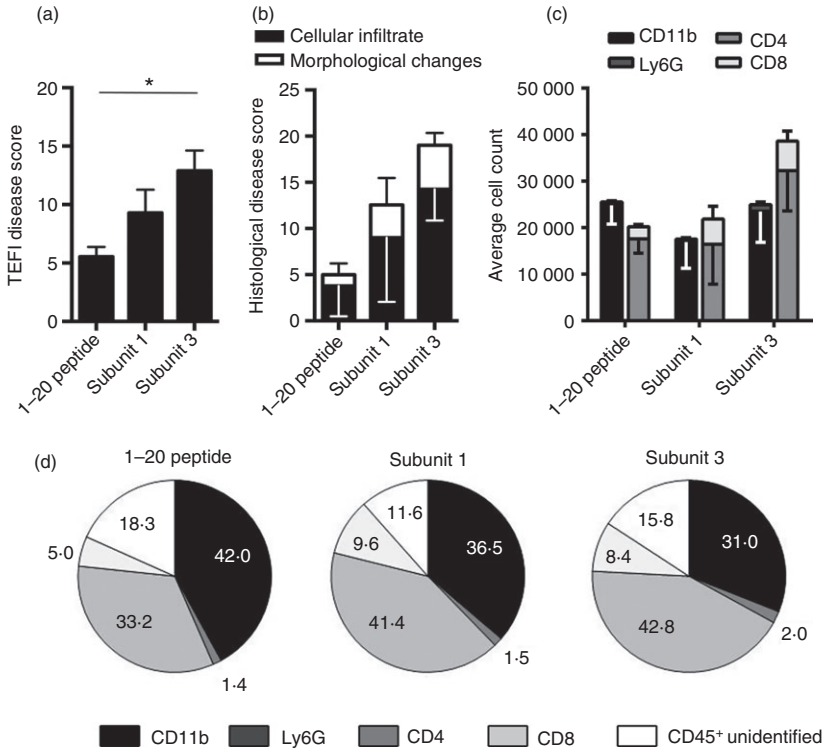

Figure 2. Recombinant subunit 3 induces a severe form of experimental autoimmune uveoretinitis (EAU) compared with 1–20 retinol binding protein-3 (RBP-3) peptide. C57BL/6J mice were immunized with either 50 μg/ml RBP-3 recombinant subunits 1 or 3, or 500 μg/ml 1–20 RBP-3 peptide. Clinical disease was monitored by topical endoscopic fundal imaging (TEFI) before killing and enucleation. Right eyes were snap frozen, sectioned (12 μm) and stained for $CD45^+$ infiltrate for quantification by immunohistochemistry. Left eyes were processed to quantify $CD45^+$ cell infiltrate by flow cytometry. (a) Total clinical scores determined by TEFI for all treatment groups. Data are a combination of three independent experiments. Each treatment group contains a minimum of 10 eyes. Kruskal–Wallis analysis of variance was used to determine *P* values (*$P < 0{\cdot}05$). (b) Total clinical scores of cellular infiltrate and structural damage determined by immunohistochemistry for each treatment group. Data are a combination of two independent experiments. Each treatment group has a minimum of three eyes. (c) Average cell number per retina pooled from three independent experiments for $CD45^+$ cell numbers. Markers for $CD11b^+$ macrophages, $Ly6G^+$ neutrophils and $CD4^+$ and $CD8^+$ T cells are shown. Each treatment group has a minimum of nine eyes. (d) Pie charts represent average percentages of various retinal subpopulations (CD11b, Ly6G, CD4, CD8 and unidentified population). All cells were gated on $7AAD^-CD45^+$ populations.

scores > 68 (arbitrary units) and/or identified in the library screen were then tested for pathogenicity (Table 1). We did not detect positive responses from peptides spanning residues 652–675. Four immunogenic regions were identified, and overlapping peptides from one, RBP-3 peptides 629–641 and 631–643, induced clinical EAU with signs of disease including inflammation of the optic disc region and vasculitis (Table 1).

RBP-3 peptide 629–643 is a CD4 and CD8 epitope

Having established the identity of a novel pathogenic region within subunit 3 we synthesized peptide 629–643 (EAHYARPEIAQRARA), which spanned the full length of this epitope. Mice were immunized with RBP-3 629–643 and splenocytes were prepared to measure T-cell responses. As anticipated there was a significant ($P < 0{\cdot}01$) antigen-specific response compared with the OVA peptide control, measured both by proliferation (Fig. 3a) and by cytokine production of IFN-γ and IL-17 (Fig. 3b). To determine the phenotype of the responding cells induced by immunization with RBP-3 629–643 we used CFSE labelling and demonstrated that the peptide encompassed both a $CD4^+$ and $CD8^+$ T-cell epitope, as in both T-cell compartments there was a significant response to the antigen compared with OVA control (Fig 3c; $P < 0{\cdot}01$, $P < 0{\cdot}05$, respectively). This is consistent with previous work demonstrating $CD4^+$ and $CD8^+$ T-cell activation following immunization with RBP-3 1–20 peptide.[5,19]

RBP-3 peptide 629–643 induces EAU

Next we characterized the disease that peptide 629–643 induced by clinical assessment, analysis of the morphological and structural damage to the retina by immunohistochemistry and multiparameter phenotyping of cellular infiltrate. Figure 4 demonstrates that RBP-3 derived 629–643 peptide induces a typical EAU pheno-

Table 1. Peptide library sequences

Peptide	Peptide sequence		Immunogenic	Cellular infiltrate	Pathogenic
623–635	Murine	GTGRLLEAHYARP	Y	–	–
	Human	GTGHLLEAHYARP			
	Bovine	GTGRLLEAHYARP			
629–641	Murine	EAHYARPEIAQRA	Y	Y	Y
	Human	EAHYARPEVVGQT			
	Bovine	EAHYARPEVVGQM			
631–643	Murine	HYARPEIAQRARA	Y	Y	Y
	Human	HYARPEVVGQTSA			
	Bovine	HYARPEVVGQMGA			
647–659	Murine	SKLAQGAYRTAVD	–	–	–
	Human	AKLAQGAYRTAVD			
	Bovine	AKLAQGAYRTAVD			
652–664	Murine	GAYRTAVDLESLA	Y	–	–
	Human	GAYRTAVDLESLA			
	Bovine	GAYRTAVDLESLA			
672–684	Murine	QEVSEDHRLLVFH	–	–	–
	Human	QEVSGDHRLLVFH			
	Bovine	QEMSGDHRLLVFH			
681–693	Murine	LVFHSPGELVAEE	–	–	–
	Human	LVFHSPGELVVEE			
	Bovine	LVFHSPGEMVAEE			
700–712	Murine	AVPSPEELSYLIE	–	–	–
	Human	AVPSPEELTYLIE			
	Bovine	VVPSPEELSYLIE			
779–791	Murine	SYFFEAEPRQHLY	Y	–	–
	Human	SYFFEAEPRQHLY			
	Bovine	SYFFEAEPRRHLY			
832–844	Murine	AAEAFAHTMQDLQ	Y	–	–
	Human	AAEAFAHTMQDLQ			
	Bovine	AAEAFAHTMQDLQ			
850–862	Murine	GEPTAGGALSVGI	–	–	–
	Human	GEPTAGGALSVGI			
	Bovine	GEPTAGGALSVGI			
880–892	Murine	LSASTGEAWDLAG	–	–	–
	Human	MSATTGKAWDLAG			
	Bovine	MSASTGEAWDLAG			
896–908	Murine	DITVPMSEALSTA	–	–	–
	Human	DITVPMSEALSIA			
	Bovine	DITVPMSVALSTA			

Y, yes, –, no.

Sequences for human and bovine RBP-3 from Ref. 18. Non-conserved amino acids are underlined. Pathogenic peptides are highlighted in gray.

type with inflamed optic disc, retinal vasculitis and choroidal lesions (Fig. 4a). Clinical scoring of the retina showed that EAU induced by peptide 629–643 was of comparable severity to that of RBP-3 1–20 induced EAU (Fig. 4b–d, Table 2).[5] Furthermore, the incidence of disease in animals immunized with either peptide is equivalent, although a little lower than was seen in animals immunized with recombinant subunits (Table 2). As expected, flow cytometry on the retina of animals with EAU revealed dominant populations of $CD11b^+$ macrophages and $CD4^+$ T cells (Fig. 4e,f). In the $CD8^+$ T-cell compartment, as previously reported for disease induced with RBP-3 1–20,[5] just less than 10% of the infiltrating $CD45^+$ population were $CD8^+$ T cells at the primary peak of disease (Fig. 4e,f). As disease progressed the percentage of $CD8^+$ T cells increased (Fig. 4f,h). This expansion has been previously documented in both the murine C57BL/6J EAU and rat EAU models.[5,20]

Peptide-induced EAU leads to epitope spreading in C57BL/6J animals

The identification of a new pathogenic peptide that induced disease of equal severity and potency as peptide

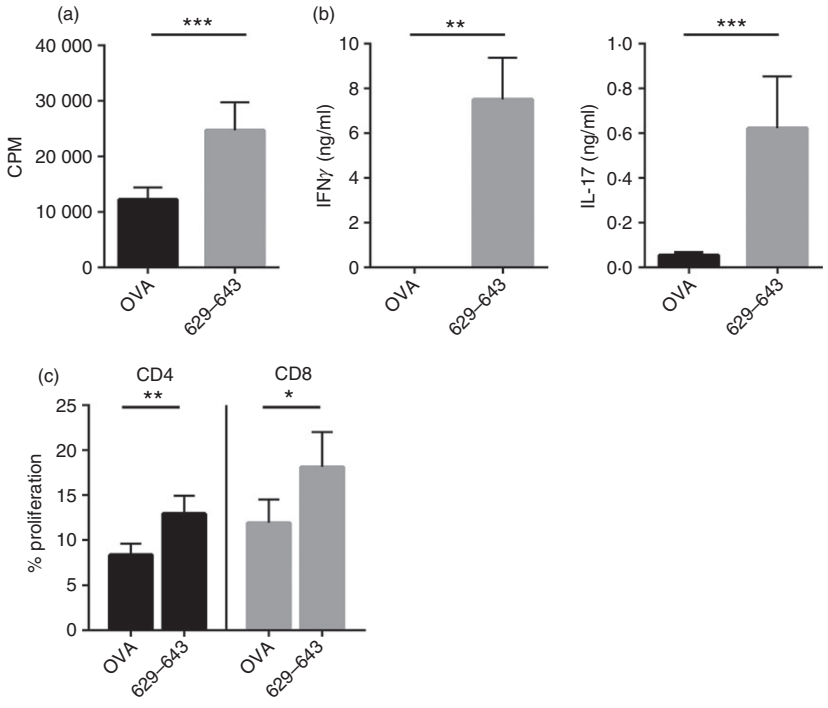

Figure 3. $CD4^+$ and $CD8^+$ T cells respond to retinol binding protein-3 (RBP-3) peptide 629–643. C57BL/6J mice were immunized with 400 μg 629–643 RBP-3 peptide and at days 21–27 after immunization spleens were taken to measure proliferation by thymidine incorporation or CFSE dilution. (a) Proliferation from splenocytes measured by thymidine incorporation following stimulation with either ovalbumin (OVA) peptide or 629–643 peptide. Data are represented as average counts/min ± SEM per animal, assays performed in triplicate. (b) Interferon-γ (IFNγ) and interleukin-17 (IL-17) production from splenocyte cultures were detected by ELISA. (c) Proliferation from splenocytes measured by CFSE incorporation. All splenocytes were subsequently stained to mark $CD4^+$ and $CD8^+$ T cells, all cells gated on 7AAD negative populations. Data represents at least four independent experiments, with at least four mice in each group presented as mean ± SEM. Wilcoxon Signed Ranked test was used to determine *P* values, $*P < 0{\cdot}05$, $**P < 0{\cdot}01$, $***P = <0{\cdot}001$.

1–20, allowed us to study epitope spreading. Epitope spreading is an important contributor to clinical disease progression in a number of models of autoimmune disease.[21,22] There have been limited reports of intramolecular epitope spreading in uveitis in the rat and equine model of EAU.[23,24] To determine whether priming with one peptide produced detectable responses to a second RBP-3 epitope, C57BL/6J mice were immunized with either RBP-3 1–20 or 629–643 peptide; splenocytes were prepared and *in vitro* proliferation responses to OVA peptide and RBP-3 peptides 629–643 or 1–20 were determined (Fig. 5a–d). Following immunization with either peptide, we were able to detect significant immune responses directed towards the non-immunizing determinant, which was observed by days 21–25 ($P < 0{\cdot}01$). This response remained detectable at later time points (days 40–45; $P < 0{\cdot}05$). This is explained by a model in which in the C57BL/6J mouse the destruction of retinal tissue liberates antigen in a form able to induce responses from naive T-cell populations to new epitopes derived from the effected tissue. To test whether epitope spreading was associated with disease severity and tissue damage we examined correlations between different measures of clinical disease and responses to the non-immunizing antigen. As expected and reported in EAU in other mouse strains,[14] histological scores and clinical scores were positively correlated (Fig. 5e; $r = 0{\cdot}78$, $P < 0{\cdot}001$). We then examined the individual T-cell responses from mice immunized with RBP-3 629–643 peptide and recalled with the immunizing antigen and the non-immunizing peptide. Both the immunizing peptide (629–643) and the epitope to which reactivity had spread (1–20) induced proliferation that positively correlated [$r = 0{\cdot}35$ ($P < 0{\cdot}05$), $r = 0{\cdot}49$ ($P < 0{\cdot}01$)] with the level of clinical disease (Fig. 5f,g). The correlation with disease severity was stronger with the non-immunizing peptide. The findings imply that epitope spreading; tissue damage and retinal destruction all reflect the magnitude of the pathogenic T-cell response during persistent EAU.

Discussion

In the present study we identify a novel pathogenic epitope, in the C57BL/6J mouse model of EAU, which is derived from the retinal antigen RBP-3 and found within subunit 3 of the full-length protein. This peptide induces

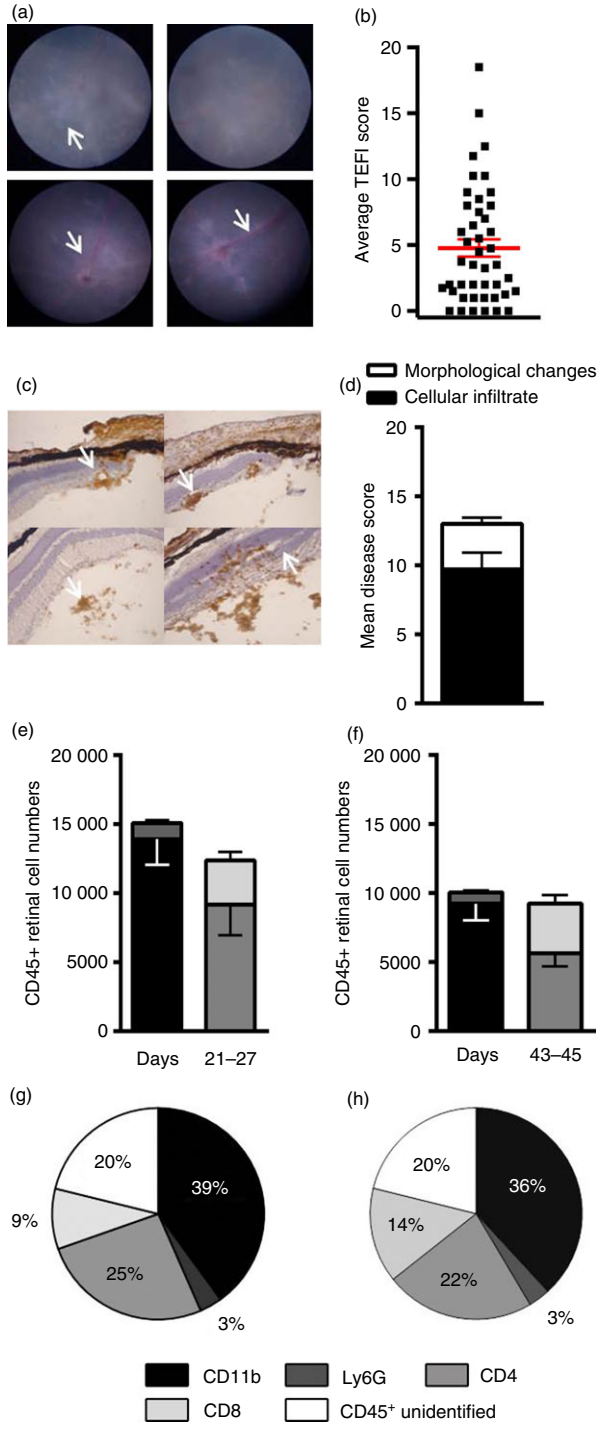

Figure 4. Retinol binding protein-3 (RBP-3) peptide 629–643 induces experimental autoimmune uveoretinitis (EAU). C57BL/6J mice were immunized with 400 μg 629–643 RBP-3 peptide after which disease progression was monitored by topical endoscopic fundal imaging (TEFI) and characterized at days 21–27 (a–d, e, g) and days 40–44 post immunization (f, h). Right eyes were snap frozen, sectioned (12 μm) and stained for $CD45^+$ infiltrate for quantification by immunohistochemistry. Left eyes were digested to quantify $CD45^+$ cell infiltrate by flow cytometry. (a) Representative TEFI images. Mice display classical features of EAU (indicated by white arrows) including inflamed optic disc, vasculitis and choroidal lesions. (b) Average EAU disease scores from TEFI images. Red line represents mean ± SEM disease score. (c) Representative histology images demonstrating structural disruption and $CD45^+$ cellular infiltrate (indicated by white arrows). (d) Average disease scores from immunohistochemical analysis. Average disease scores ± SEM are shown for morphological changes and inflammatory cellular infiltrate. (e, f) Average total CD45 cell numbers from days 21–27 and 40–45, respectively, includes markers CD11b, Ly6G, CD4 and CD8 populations. Data are expressed as mean ± SEM. (g, h) Pie charts represent average percentages of various retinal subpopulations (CD11b, Ly6G, CD4, CD8 and unidentified population). All cells were gated on $7AAD^-$ $CD45^+$ populations. Data represents four independent experiments with at least six mice in each group.

ocular inflammation and persistent disease, which has clinical features paralleling human uveitis.[3] This retinal inflammation is similar in severity to disease induced by the commonly used human peptide 1–20 (Fig. 4).[3,5] Immunizing with one peptide antigen and testing for reactivity to both pathogenic peptides allowed us to detect the epitope spreading whose presence correlates more strongly with the severity of clinical disease than does the immunizing peptide and which may therefore relate to the ongoing destructiveness of the persistent disease observed in this model.

In the initial part of this study we generated murine recombinant RBP-3 subunits, which allowed us to determine the presence of uveitogenic determinants within three of the four subunits (Fig. 1). The most severe disease was caused by RBP-3 subunit 3 and this had a destructive phenotype that was characterized by a large $CD45^+$ infiltrate, seen by both immunohistochemistry and flow cytometry (Figs 1 and 2). This clinical phenotype was more dramatic that has been reported for peptide 651–670 raising the possibility that other pathogenic epitopes might be detectable in subunit 3. To investigate, a peptide library of overlapping peptides based on the murine sequence was designed to identify the dominant pathogenic epitope. Previously, studies have used a combination of bovine and human RBP-3 sequences,[12] and this new analysis identified the 629–643 RBP-3 epitope in a region of low amino acid homology between the murine, bovine and human sequences, which explains why this epitope was not detected previously (Table 1). However, the highly destructive form of EAU induced by subunit 3 was not recapitulated by immunizing peptide 629–643 alone. The differences in tissue folding and granuloma formation could be because there are other pathogenic epitopes within subunit 3 that we overlooked in this study that may contribute to this phenotype or relate to the presence of innate immune ligands in the purified recombinant protein that have additional adjuvant properties influencing disease severity, or to

Table 2. Experimental autoimmune uveoretinitis (EAU) incidence and disease scores for C57BL/6 mice

Strain	Immunizing antigen	Incidence (%)	Average TEFI score (±SEM)
C57BL/6J	RBP-3 subunit 1	90	2·3 ± 0·5
C57BL/6J	RBP-3 subunit 3	90	3·2 ± 0·4
C57BL/6J	RBP-3 1–20 peptide	85	1·4 ± 0·2
C57BL/6J	RBP-3 629–643 peptide	84	1·2 ± 0·2

Disease scores from topical endoscopic fundal imaging (TEFI) analysis are represented as mean ± SEM. Disease incidence is the number of mice with EAU out of the number of mice in each treatment group expressed as an average percentage

differences in the processing and presentation of peptides from larger recombinant proteins compared with synthetic peptides that do not require antigen-presenting cell processing.[25] Using our shorter peptide library (15mers rather than 20mers) we did not detect pathogenicity within the 651–670 region previously shown to be uveitogenic.[12] This probably reflects the effects that peptide length can have on immunogenicity[26] and emphasizes the relevance of processing to the heightened pathogenicity of subunit 3.

Previous reports have found that the RBP-3 1–20 epitope encompasses epitopes recognized by both $CD4^+$ and $CD8^+$ T cells.[19] Strikingly, we also found that both $CD4^+$ and $CD8^+$ T-cell populations included cells that responded in an antigen-specific fashion to the 629–643 RBP-3 peptide. In support of a role for the $CD8^+$ T-cell-specific response we demonstrated a significant $CD8^+$ T-cell population in the retina throughout disease and the expansion of this population as a fraction of the total cell infiltrate in late-stage EAU, which corroborates our previous data.[5] Furthermore, the EAU induced by 629–643 RBP-3 had similar proportions of the other cellular subpopulations when compared with RBP-3 1–20 induced EAU, although slightly fewer $CD45^+$ leucocytes in total, which can be accounted for by a greater variability in the severity of disease.

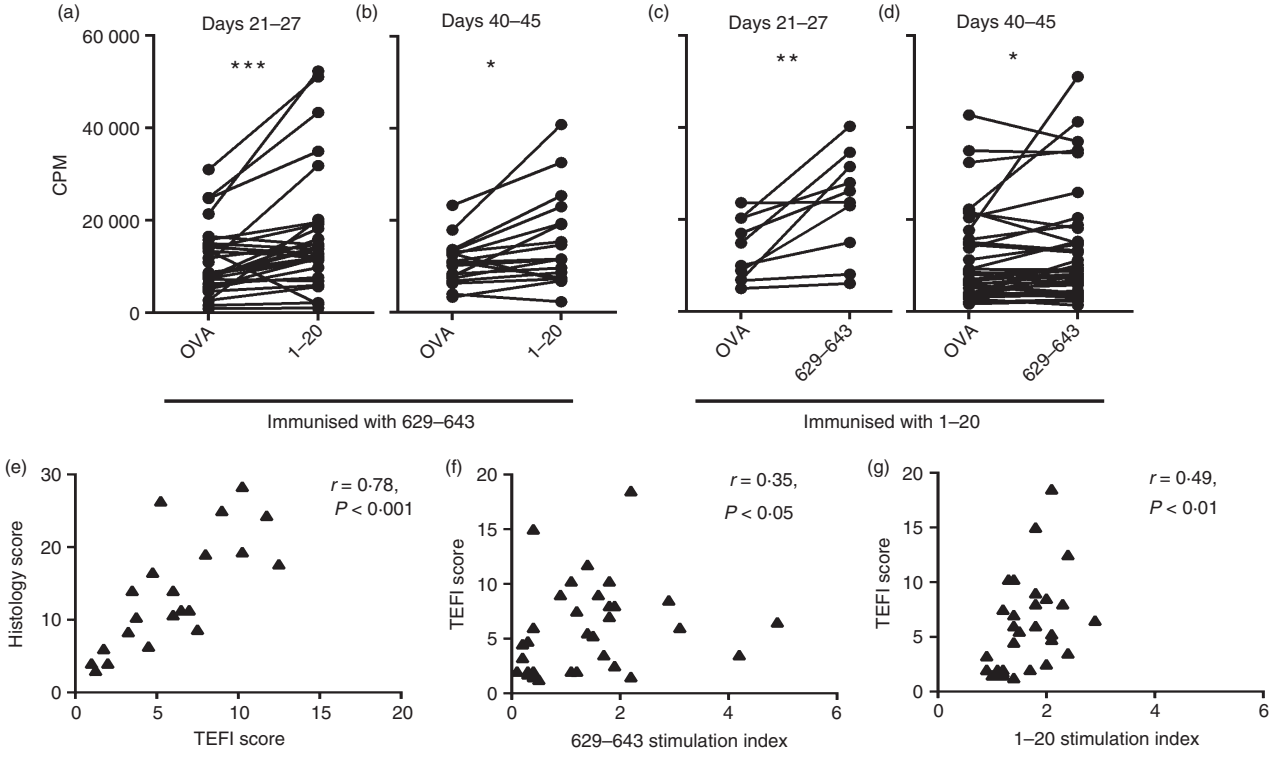

Figure 5. The 629–643 induced experimental autoimmune uveoretinitis (EAU) is accompanied by epitope spreading to retinol binding protein-3 (RBP-3)1–20. C57BL/6J mice were immunized with equimolar 629–643 or 1–20 RBP-3 peptide and at days 21–27 or days 40–45 post immunization proliferation was measured in the spleens by thymidine incorporation. (a, b) Proliferation of splenocytes following stimulation with either ovalbumin (OVA) or 1–20 RBP-3 peptides after immunization with 629–643 RBP-3. (c, d) Proliferation of splenocytes following stimulation with either OVA or 629–643 RBP-3 peptide after immunization with 1–20 RBP-3. Data are represented as average counts/min (cpm) per animal performed in triplicate. Data are pooled from at least two independent experiments, with at least five animals in each group. $*P < 0{\cdot}05$, $**P < 0{\cdot}01$, $***P = <0{\cdot}001$ (Wilcoxon Signed Rank sum). (e) Clinical disease [topical endoscopic fundal imaging (TEFI) score] and histology score are strongly correlated in animals immunized with RBP-3 629–643. (f, g) Stimulation index relative to OVA control correlates significantly with TEFI score at time of assay recalled with immunizing (RBP-3 629–643) or non-immunizing (RBP-3 1–20) peptide. The correlation of disease score with the non-immunizing peptide is stronger than with the immunizing peptide ($r = 0{\cdot}49$ versus 0·35; Spearman correlation).

Epitope spreading is an important component of pathogenicity in models of autoimmune disease.[22,27] For the first time we demonstrate this process in a mouse model of persistent experimental autoimmune uveitis. The presence of many disease causing epitopes within RBP-3 may be part of the explanation for the crucial role that it plays in ensuring immune tolerance to ocular tissue.[9] Our demonstration of epitope spreading correlated with clinical disease is consistent with this important role and implies an evolving immune response as an important part of the process of chronic autoimmune ocular inflammation. In this model epitope spreading to the non-immunizing peptide was demonstrated for both RBP-3 1–20 and RBP-3 629–643. This is consistent with the destruction of retinal tissue increasing the size of the antigen-specific effector T-cell repertoire as disease progresses. The correlation between reactivity to the non-immunizing epitope and clinical disease (Fig. 5) is also supportive of increased reactivity to more determinants playing a part in the severity of disease. This has been described in an equine model of recurrent uveitis, where intramolecular spreading was demonstrated and could be seen to correlate to relapsing episodes of disease.[24] In EAE epitope spreading has been extensively characterized and has been shown to have a pathological role in chronic progression of disease.[22,28] This was also demonstrated in a restricted humanized transgenic EAE mouse model, where it was shown that mice that developed severe disease showed enhanced responses to a wider range of peptides compared with mice with minimal paralysis.[29] All this work reinforces the likelihood that epitope spreading will be a component of uveitis in other mouse strains.

Spreading to new epitopes is clearly only one component of the disease process, as we observed significant variability in the immune response towards the spreading determinant when the response was analysed in spleen cells. Several possible mechanisms may account for this; first it may be that some mice have less tissue damage and this limits expansion in the T-cell repertoire. Second, it is possible that other epitopes, which may be released by tissue damage, compete for available resources and alter patterns of T-cell reactivity. In EAE there is some evidence of a hierarchy of dominance in epitope spreading[21] but it is not known if this is the case in uveitis. Third, detecting immune responses in the spleen may not completely correlate with what occurs in the tissue; to address this other techniques to examine responding T-cell populations may need to be developed. Finally, it is possible that in some mice, the regulation of specific immune responses contributes to the lack of detection of epitope spreading both in the spleen and potentially also in the ocular tissue.

In conclusion, we describe a new pathogenic epitope in the C57BL/6J mouse model of EAU and demonstrate a correlation between reactivity to a broader autoimmune repertoire and clinical disease that may reflect the underlying severity of the disease process.

Acknowledgements

This work was funded by the National Eye Research Centre (NERC). We thank Dr Jim Spencer for assistance with the production of recombinant proteins.

Disclosures

All authors declare no competing interests.

References

1 Imrie FR, Dick AD. Biologics in the treatment of uveitis. *Curr Opin Ophthalmol* 2007; **18**:481–6.
2 Kerr EC, Raveney BJ, Copland DA, Dick AD, Nicholson LB. Analysis of retinal cellular infiltrate in experimental autoimmune uveoretinitis reveals multiple regulatory cell populations. *J Autoimmun* 2008; **31**:354–61.
3 Chen M, Copland DA, Zhao J, Liu J, Forrester JV, Dick AD *et al.* Persistent inflammation subverts thrombospondin-1-induced regulation of retinal angiogenesis and is driven by CCR2 ligation. *Am J Pathol* 2012; **180**:235–45.
4 Avichezer D, Silver PB, Chan CC, Wiggert B, Caspi RR. Identification of a new epitope of human IRBP that induces autoimmune uveoretinitis in mice of the H-2(b) haplotype. *Invest Ophthalmol Vis Sci* 2000; **41**:127–31.
5 Boldison J, Chu CJ, Copland DA, Lait PJP, Khera TK, Dick AD *et al.* Tissue-resident exhausted effector memory CD8+ T cells accumulate in the retina during chronic experimental autoimmune uveoretinitis. *J Immunol* 2014; **192**:4541–50.
6 Guyver CJ, Copland DA, Calder CJ, Sette A, Sidney J, Dick AD *et al.* Mapping immune responses to mRBP-3 1-16 peptide with altered peptide ligands. *Invest Ophthalmol Vis Sci* 2006; **47**:2027–35.
7 Lee RW, Nicholson LB, Sen HN, Chan CC, Wei L, Nussenblatt RB *et al.* Autoimmune and autoinflammatory mechanisms in uveitis. *Semin Immunopathol* 2014; **36**:581–94.
8 Egwuagu CE, Charukamnoetkanok P, Gery I. Thymic expression of autoantigens correlates with resistance to autoimmune disease. *J Immunol* 1997; **159**:3109–12.
9 DeVoss J, Hou Y, Johannes K, Lu W, Liou GI, Rinn J *et al.* Spontaneous autoimmunity prevented by thymic expression of a single self-antigen. *J Exp Med* 2006; **203**:2727–35.
10 Avichezer D, Grajewski RS, Chan CC, Mattapallil MJ, Silver PB, Raber JA *et al.* An immunologically privileged retinal antigen elicits tolerance: Major role for central selection mechanisms. *J Exp Med* 2003; **198**:1665–76.
11 Caspi RR, Grubbs BG, Chan CC, Chader GJ, Wiggert B. Genetic-control of susceptibility to experimental autoimmune uveoretinitis in the mouse model - concomitant regulation by Mhc and Non-Mhc Genes. *J Immunol* 1992; **148**:2384–9.
12 Cortes LM, Mattapallil MJ, Silver PB, Donoso LA, Liou GI, Zhu W *et al.* Repertoire analysis and new pathogenic epitopes of IRBP in C57BL/6 (H-2b) and B10.RIII (H-2r) mice. *Invest Ophthalmol Vis Sci* 2008; **49**:1946–56.
13 Mattapallil MJ, Wawrousek EF, Chan CC, Zhao H, Roychoudhury J, Ferguson TA *et al.* The Rd8 mutation of the Crb1 gene is present in vendor lines of C57BL/6N mice and embryonic stem cells, and confounds ocular induced mutant phenotypes. *Invest Ophthalmol Vis Sci* 2012; **53**:2921–7.
14 Copland DA, Wertheim MS, Armitage WJ, Nicholson LB, Raveney BJE, Dick AD. The clinical time-course of experimental autoimmune uveoretinitis using topical endoscopic fundal imaging with histologic and cellular infiltrate correlation. *Invest Ophthalmol Vis Sci* 2008; **49**:5458–65.
15 Xu H, Koch P, Chen M, Lau A, Reid DM, Forrester JV. A clinical grading system for retinal inflammation in the chronic model of experimental autoimmune uveoretinitis using digital fundus images. *Exp Eye Res* 2008; **87**:319–26.
16 Copland DA, Liu J, Schewitz-Bowers LP, Brinkmann V, Anderson K, Nicholson LB *et al.* Therapeutic Dosing of Fingolimod (FTY720) prevents cell infiltration, rapidly suppresses ocular inflammation, and maintains the blood-ocular barrier. *Am J Pathol* 2012; **180**:672–81.
17 Namba K, Kitaichi N, Nishida T, Taylor AW. Induction of regulatory T cells by the immunomodulating cytokines alpha-melanocyte-stimulating hormone and transforming growth factor-beta 2. *J Leukoc Biol* 2002; **72**:946–52.
18 Shuler RK, Gross E, He WY, Liou GI, Nickerson JM. Sequence analysis of the mouse IRBP gene and cDNA. *Curr Eye Res* 2002; **24**:354–67.

19 Shao H, Peng Y, Liao T, Wang M, Song M, Kaplan HJ *et al.* A shared epitope of the interphotoreceptor retinoid-binding protein recognized by the CD4+ and CD8+ autoreactive T cells. *J Immunol* 2005; **175**:1851–7.
20 Chan CC, Mochizuki M, Nussenblatt RB, Palestine AG, Mcallister C, Gery I *et al.* Lymphocyte-T subsets in experimental autoimmune uveitis. *Clin Immunol Immunopathol* 1985; **35**:103–10.
21 Yu M, Johnson JM, Tuohy VK. A predictable sequential determinant spreading cascade invariably accompanies progression of experimental autoimmune encephalomyelitis: a basis for peptide-specific therapy after onset of clinical disease. *J Exp Med* 1996; **183**:1777–88.
22 Vanderlugt CL, Miller SD. Epitope spreading in immune-mediated diseases: implications for immunotherapy. *Nat Rev Immunol* 2002; **2**:85–95.
23 Diedrichs-Mohring M, Hoffmann C, Wildner G. Antigen-dependent monophasic or recurrent autoimmune uveitis in rats. *Int Immunol* 2008; **20**:365–74.
24 Deeg CA, Amann B, Raith AJ, Kaspers B. Inter- and intramolecular epitope spreading in equine recurrent uveitis. *Invest Ophthalmol Vis Sci* 2006; **47**:652–6.
25 DiPaolo RJ, Unanue ER. Cutting edge: chemical dominance does not relate to immunodominance: studies of the CD4+ T cell response to a model antigen. *J Immunol* 2002; **169**:1–4.
26 Carson RT, Vignali KM, Woodland DL, Vignali DA. T cell receptor recognition of MHC class II-bound peptide flanking residues enhances immunogenicity and results in altered TCR V region usage. *Immunity* 1997; **7**:387–99.
27 Lehmann PV, Forsthuber T, Miller A, Sercarz EE. Spreading of T-cell autoimmunity to cryptic determinants of an autoantigen. *Nature* 1992; **358**:155–7.
28 McMahon EJ, Bailey SL, Castenada CV, Waldner H, Miller SD. Epitope spreading initiates in the CNS in two mouse models of multiple sclerosis. *Nat Med* 2005; **11**:335–9.
29 Ellmerich S, Takacs K, Mycko M, Waldner H, Wahid F, Boyton RJ *et al.* Disease-related epitope spread in a humanized T cell receptor transgenic model of multiple sclerosis. *Eur J Immunol* 2004; **34**:1839–48.